J. Fluid Mech. (2002), *vol.* 469, *pp.* 209–235.
DOI: 10.1017/S0022112002001817 Printed in the United Kingdom

Exact solutions for rotating vortex arrays with finite-area cores

By DARREN G. CROWDY

Department of Mathematics, Imperial College of Science, Technology and Medicine, 180 Queen's Gate, London, SW7 2BZ, UK

(Received 19 April 2001 and in revised form 31 May 2002)

A class of explicit solutions of the two-dimensional Euler equations consisting of a finite-area patch of uniform vorticity surrounded by a finite distribution of co-rotating satellite line vortices is constructed. The results generalize the classic study of co-rotating vortex arrays by J. J. Thomson. For N satellite line vortices ($N \geqslant 3$) a continuous one-parameter family of rotating vortical equilibria is derived in which different values of the continuous parameter correspond to different shapes and areas of the central patch. In an appropriate limit, vortex patch equilibria with cusped boundaries are found. A study of the linear stability is performed and a wide range of the solutions found to be linearly stable. Contour dynamics methods are used to calculate the typical nonlinear evolution of the configurations. The results are believed to provide the only known exact solutions involving rotating vortex patches besides the classical Kirchhoff ellipse.

1. Introduction

Since the early work of Lord Kelvin (1878) who studied the case of three vortices arranged in a ring, vortex arrays (or vortex 'lattices' or 'crystals') have been a problem of perennial interest to fluid dynamicists. Thomson (1882) considered the more general situation in which N line vortices are arranged in a co-rotating configuration equispaced around the circumference of a circle for up to $N = 7$. This problem was later reappraised by Havelock (1931) who also considered larger values of N and corrected some erroneous conclusions made by Thomson regarding the stability of the configurations.

Generalizations of this classical work include that of Morikawa & Swenson (1971) who, in an attempt to model geostrophic vortices in the atmosphere, placed an additional line vortex at the centre of the co-rotating polygonal array of satellites. The central line vortex was a simple model of the polar vortex whereas the satellites modelled vortex cores associated with atmospheric pressure systems in the hemisphere surrounding the pole. Further applications of this model to atmospheric pressure systems were considered later by Bauer & Morikawa (1976).

Motivated by the formation of finite vortex arrays in superfluid helium (e.g. Yarmchuk, Gordon & Packard 1979), Campbell & Ziff (1978) have constructed a catalogue of stable line vortex equilibria for up to $N = 50$ line vortices. Research into line vortex equilibria of this kind continues. For example, Aref (1998) and co-workers have recently discovered a class of line vortex equilibria which seem to lack any form of symmetry.

Dritschel (1985, 1986) has considered rather different generalizations of Thomson's

co-rotating arrays of line vortices. By replacing the line vortices by patches of uniform vorticity, he constructed a class of equilibria consisting of co-rotating vortex patches. These equilibria were computed numerically. Having calculated the equilibrium solutions, Dritschel (1985) went on to study the linear and nonlinear (Dritschel 1986) stability of the solutions. Polvani & Dritschel (1993) have discussed models of the polar vortex using configurations of line vortices and patches on the surface of a sphere.

Even more recently, there has been experimental interest in these vortex patterns. Durkin & Fajans (2000) have studied the formation and stability of the N vortices in a ring, as well as the Morikawa & Swenson problem with a central vortex, in a Malmberg–Penning trap. A strongly magnetized electron column can be described, in appropriate circumstances, by the two-dimensional drift-Poisson equations which are isomorphic to the two-dimensional Euler equations. The formation of stable vortex patterns in a Malmberg–Penning trap was first reported by Fine *et al.* (1995) and has again prompted renewed interest in stable vortical equilibria.

In this paper, we make a contribution to the understanding of equilibrium vortex arrays by considering a generalization of Thomson's co-rotating line vortex problem in which a finite-area patch of uniform vorticity is placed with its centroid at the centre of the co-rotating configuration. To the best of my knowledge, this problem has not been previously studied in the literature, even by numerical means. It turns out that a class of exact mathematical solutions to this problem can be written down in closed form. These solutions are presented here. The solutions can be understood as bifurcating, in an appropriate sense, from the classical Rankine vortex (Saffman 1992).

Given the basic nature of the problem of vortex dynamics under consideration, this paper limits itself to a general and non-specific derivation of the solutions and a study of their stability properties. The range of possible applications and uses of the new exact solutions is potentially broad. Vortex arrays arise in a number of disparate applications including studies of superfluid helium (Yarmchuk *et al.* 1979; Acheson 1990) and magnetically confined electron columns (Fine *et al.* 1995; Durkin & Fajans 2000). There are analogies between the vorticity equation of ideal inviscid fluids and the Vlasov equation of charged particle physics and it is possible that the exact solutions presented herein might have corresponding analogues in the 'water bag' method for calculating phase space evolution problems of plasma physics (see Pullin 1992 for a list of references). The solutions also provide more realistic models of the polar vortex than the line vortex models considered by Morikawa & Swenson (1971) and Bauer & Morikawa (1976). Bauer & Morikawa (1976) realize this deficiency in their model and suggest that a more realistic one might be obtained by replacing the single polar vortex by a stable $3 + 1$ line vortex system where the centre vortex is an anticyclone surrounded by three cyclones. This is a way of increasing the degrees of freedom of the model in describing the complicated concentration of vorticity at the hemispherical pole while retaining the mathematical simplicity implicit in line vortex models. The solutions here in which the polar vortex is modelled by a finite-area vortex patch also share the virtues of mathematical exactness.

A subsidiary result of the present work involves an issue which has been the source of much discussion and controversy in the vortex dynamics literature. This is the question of the existence of equilibrium patches of uniform vorticity with cusp singularities in their boundaries. In a limiting case, the central vortex patches in the exact solution class presented here are found to admit such cusp singularities. Overman (1986) has shown that a discontinuous tangent angle in the boundary

of an equilibrium vortex patch (or 'V-state') can only jump by either 90° or 180°. He also surveyed the extant literature and, applying a combined local and global method, discovered that all known limiting equilibria correspond to corner formation. Overman (1986) found no situation admitting cusps even though there had been statements in the literature that such cusps had been found numerically. See Overman (1986) for a full discussion of the debate in the literature.

Exact solutions of the Euler equations involving distributions of vorticity with dense support are rare, so it seems appropriate to document any such solutions. Non-trivial exact solutions can provide important bench-marks for checking numerical codes. To the best of my knowledge, the solutions derived herein are the only examples, besides the classical Kirchhoff ellipse (Saffman 1992), of mathematically exact equilibria of the Euler equations involving rotating finite patches of non-zero vorticity.

In § 2, the mathematical construction of the exact equilibria is described. In § 3, the linear stability of the solutions is studied using a spectral method based on Taylor and Laurent series. Finally, in § 4, a brief study of the nonlinear evolution of some typical equilibria is presented.

2. Exact rotating equilibria

Consider the classical Rankine vortex solution (Saffman 1992) of the steady two-dimensional Euler equations governing an ideal inviscid fluid. The velocity field is purely azimuthal and is given in cylindrical polar coordinates as $\boldsymbol{u} = (0, V(r))$ where

$$V(r) = \begin{cases} \frac{1}{2}\omega r, & r \leqslant a, \\ \dfrac{1}{2r}\omega a^2, & r > a. \end{cases} \tag{2.1}$$

This flow consists of a circular patch of radius a and uniform vorticity ω surrounded by irrotational flow everywhere outside the patch.

The fact that the Rankine vortex solution consists of a finite-area patch which not only has constant vorticity, but is also in pure solid-body rotation, provides the basis of our method of generalization. If (u, v) denote the Cartesian components of the velocity of the Rankine vortex, then we can alternatively write the solution (2.1) in terms of the complex variable $z = x + \mathrm{i}y$ (where x and y are the usual Cartesian coordinates) as

$$u - \mathrm{i}v = \begin{cases} -\frac{1}{2}\mathrm{i}\omega\bar{z}, & z \in D, \\ -\frac{1}{2}\mathrm{i}\omega S(z), & z \notin D, \end{cases} \tag{2.2}$$

where

$$S(z) \equiv \frac{a^2}{z}, \tag{2.3}$$

and where D denotes the closed circular disk $|z| \leqslant a$. It is important to make the observation that $S(z)$ coincides with what is known as the Schwarz function (see Davis 1974) of the curve ∂D bounding the region D of constant vorticity that is in solid-body rotation. In this case, ∂D is a circle of radius a.

The Schwarz function $S(z)$ of an arbitrary analytic curve ∂D is defined to be the function which is analytic in an annulus containing ∂D and which satisfies

$$S(z) = \bar{z} \quad \text{on } \partial D. \tag{2.4}$$

The general theory of the Schwarz function is discussed by Davis (1974). In the

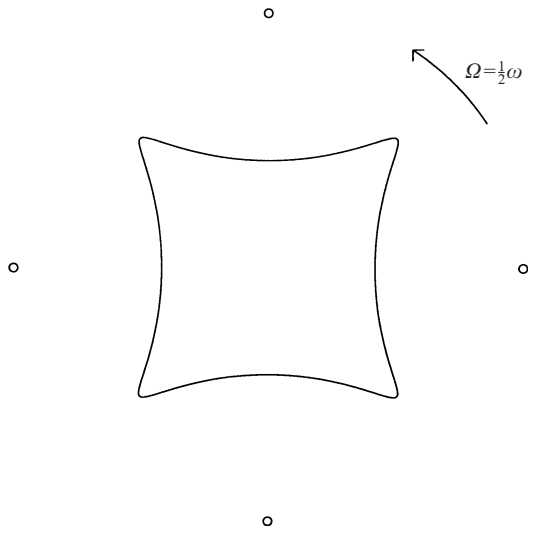

FIGURE 1. The typical vorticity distribution of interest: a four-fold symmetric central uniform vortex patch of vorticity ω rotating with angular velocity $\Omega = \frac{1}{2}\omega$ with four co-rotating satellite line vortices (shown as small circles).

example of a circular disk of radius a, the equation of the circular boundary is given by

$$z\bar{z} = a^2, \tag{2.5}$$

so that, everywhere on the boundary,

$$\bar{z} = \frac{a^2}{z}. \tag{2.6}$$

Thus, $S(z)$ as given in (2.3) is indeed the Schwarz function of the circle.

In a frame of reference co-rotating with the patch of vorticity in solid-body rotation, the velocity field can be written

$$u - \mathrm{i}v = \begin{cases} 0, & z \in D, \\ -\frac{1}{2}\mathrm{i}\omega S(z) + \frac{1}{2}\mathrm{i}\omega\bar{z}, & z \notin D. \end{cases} \tag{2.7}$$

In the case of the Rankine vortex, the patch D has a trivial geometrical structure, i.e. it is a circular disk. We now seek solutions in which a finite-area patch of uniform vorticity ω, with non-trivial geometrical structure, is in solid-body rotation with angular velocity $\frac{1}{2}\omega$ and is surrounded by a finite distribution of line vortices which rotate with the same angular velocity. This situation is shown in figure 1. In this paper, attention is restricted to configurations having N-fold rotational symmetries. Except for the set of line vortices, the flow everywhere exterior to the central patch is assumed to be irrotational. If there are N line vortices of strength Γ_j at points $\{z_j | j = 1, \ldots, N\}$ then, in a co-rotating frame of reference, the complex velocity field has the form:

$$u - \mathrm{i}v = \begin{cases} 0, & z \in D, \\ \displaystyle\sum_{j=1}^{N} -\frac{\mathrm{i}\Gamma_j}{2\pi(z - z_j)} + \mathrm{i}F(z) + \frac{1}{2}\mathrm{i}\omega\bar{z}, & z \notin D, \end{cases} \tag{2.8}$$

where the velocity field, and the domain D, are independent of time and $F(z)$ is

analytic everywhere outside D decaying to zero as $|z| \to \infty$. The flow inside D vanishes identically because the fluid in D is in solid-body rotation.

To examine whether non-trivial solutions of the form (2.8) can be found, consider a streamfunction defined by

$$\psi = \begin{cases} 0, & z \in D, \\ \frac{1}{4}\omega \left[z\bar{z} - \displaystyle\int^{z} S(z')\,\mathrm{d}z' - \int^{\bar{z}} \bar{S}(z')\,\mathrm{d}z' \right], & z \notin D. \end{cases} \tag{2.9}$$

where D is now some arbitrary patch of uniform vorticity in solid-body rotation and $S(z)$ is the Schwarz function of its boundary ∂D which is assumed to be an analytic curve.

First, it is necessary to determine whether all the dynamical constraints of the Euler equation can be satisfied on the boundary of the patch. There is a dynamical condition that the fluid velocities everywhere on the patch boundary ∂D must be continuous. This is known to be equivalent (Saffman 1992) to continuity of fluid pressure at the vortex jump. Approaching the patch boundary from the exterior,

$$u - \mathrm{i}v = 2\mathrm{i}\psi_z = \tfrac{1}{2}\mathrm{i}\omega(\bar{z} - S(z)), \tag{2.10}$$

on ∂D, but this is exactly zero everywhere on ∂D (and therefore equal to the interior velocity field) by definition of the Schwarz function. Because the flow inside the patch is quiescent then the fluid velocities are indeed continuous at the patch boundary.

There is a further kinematic condition on ∂D which says that, in the co-rotating frame, the boundary ∂D must be a streamline. If ψ denotes the streamfunction in the co-rotating frame then

$$\begin{aligned} 2\mathrm{i}\,\mathrm{d}\psi &= 2\mathrm{i}\psi_z\,\mathrm{d}z + 2\mathrm{i}\psi_{\bar{z}}\,\mathrm{d}\bar{z} = (u - \mathrm{i}v)\,\mathrm{d}z - (u + \mathrm{i}v)\,\mathrm{d}\bar{z} \\ &= \tfrac{1}{2}\mathrm{i}\omega(\bar{z} - S(z))\,\mathrm{d}z + \tfrac{1}{2}\mathrm{i}\omega(z - \bar{S}(\bar{z}))\,\mathrm{d}\bar{z} = 0 \quad \text{on } \partial D, \end{aligned} \tag{2.11}$$

where the last equality again follows from the definition of the Schwarz function. Thus, both the dynamic and kinematic boundary conditions on the boundary of the vortex patch are indeed satisfied by (2.9).

No specifications have yet been made on the shape of the patch D. It is a fact following from the general theory (Davis 1974) that the Schwarz function of a general analytic curve ∂D is only guaranteed to be analytic in an annular neighbourhood enclosing ∂D. If we move out of this annulus of analyticity (perhaps out to infinity, for example) then, in general, we will encounter singularities of the Schwarz function so that the velocity field (2.9) will exhibit unphysical singularities at any such points. In this way, (2.9) will not necessarily represent a consistent, physically meaningful solution of the two-dimensional Euler equation.

Suppose, however, that a very special patch D can be chosen such that the continuation of the Schwarz function $S(z)$ of ∂D everywhere outside D is purely meromorphic with a finite distribution of simple pole singularities with real residues. Mathematically, this means $S(z)$ can be written as

$$-\tfrac{1}{2}\omega S(z) = \sum_{j=1}^{N} -\frac{\gamma_j}{2\pi(z - z_j)} + f(z), \tag{2.12}$$

where $f(z)$ is analytic everywhere outside D, $\{z_j \,|\, j = 1, \ldots, N\}$ are points strictly outside D and the numbers $\{\gamma_j \,|\, j = 1, \ldots, N\}$ are real. Physically, by imposing that the velocity field is given by (2.9), condition (2.12) corresponds to exactly the situation

of interest, i.e. a uniform patch of fluid in solid-body rotation surrounded by a finite distribution of line vortex singularities. To see this, observe that the velocity field (2.9) with $S(z)$ of the form (2.12) is of exactly the required form (2.8). Moreover, the line vortices have strengths $\Gamma_j = \gamma_j$.

There are additional constraints, however. For a consistent steady solution of the two-dimensional Euler equation, it remains to ensure that each of the N line vortices at points z_j in the flow remain stationary. It is known from the Helmholtz vortex theorems (Saffman 1992) that line vortices move with the local non-self-induced velocity. This steadiness condition therefore amounts to ensuring that the non-self-induced terms in a local expansion of the velocity field about each of the points z_j is zero.

2.1. *Conformal mapping*

It is now shown, by explicit construction, that vortex patches D with boundaries whose Schwarz functions satisfy (2.12) do, in fact, exist. A convenient way to parameterize the boundaries of such patches is to consider a conformal map $z(\zeta)$ from the interior of the unit circle in a parametric ζ-plane to the exterior of the region D in the co-rotating frame.

Consider the class of conformal maps given, for each integer $N \geqslant 2$, by

$$z(\zeta) = R\left(\frac{1}{\zeta} + \frac{b\zeta^{N-1}}{\zeta^N - a^N}\right). \tag{2.13}$$

This map depends on three continuous parameters a, b and R which are assumed to be real. R represents a normalization degree of freedom, while we must have $a > 1$ in order that the conformal map be analytic everywhere inside $|\zeta| \leqslant 1$. It is also necessary that the mapping (2.13) is a univalent (that is, one-to-one) map from the unit ζ-circle. A necessary, but not sufficient, condition is that $z_\zeta(\zeta)$ vanishes nowhere inside the unit ζ-circle. Finally, it is clear that the map (2.13) possesses an N-fold rotational symmetry about the origin, i.e. if $\zeta \mapsto \zeta \exp(2\pi\mathrm{i}/N)$ then $z \mapsto z \exp(-2\pi\mathrm{i}/N)$.

The non-trivial velocity field outside the patch D in the co-rotating frame can be written, in terms of ζ and $\bar{\zeta}$, as follows:

$$u - \mathrm{i}v = \frac{\mathrm{i}\omega R}{2}\left(\frac{1}{\bar{\zeta}} + \frac{b\bar{\zeta}^{N-1}}{\bar{\zeta}^N - a^N} - \zeta - \frac{b\zeta}{1 - \zeta^N a^N}\right), \tag{2.14}$$

using the fact that

$$S(z(\zeta)) = R\left(\zeta + \frac{b\zeta}{1 - \zeta^N a^N}\right). \tag{2.15}$$

It is clear that $S(z(\zeta))$ has only simple pole singularities at the N points

$$\zeta_j = a^{-1}\exp\left(\frac{2\pi\mathrm{i}(j-1)}{N}\right), \quad j = 1, \ldots, N. \tag{2.16}$$

If $z(\zeta)$ is a univalent map inside the unit circle, it is therefore invertible at all points inside the circle so that $S(z)$ also has just simple poles at the image points $z_j = z(\zeta_j), \quad j = 1, \ldots, N$. Physically, these correspond to line vortices. By expanding $S(z)$ about the point $z_a = z(a^{-1})$ in the physical z-plane, it can be shown after some algebra that the condition for stationarity of the line vortex at z_a is given by

$$a + \frac{ba}{1 - a^{2N}} - \frac{1}{a} + \frac{b}{2Na}\left((3 - N) + \frac{z_{\zeta\zeta}(a^{-1})}{az_\zeta(a^{-1})}\right) = 0. \tag{2.17}$$

Equation (2.17) is independent of R, but is a nonlinear algebraic relation between a and b (for each N). It is convenient to consider a to be a free parameter and to view (2.17) as an implicit equation for $b = b(a;N)$. By the N-fold rotational symmetry of the conformal map and the associated velocity field, (2.17) also ensures that the other $N-1$ symmetrically disposed line vortices are also stationary.

It turns out that (2.17) can be rearranged to form a quadratic for $b(a;N)$:

$$c_2(a;N)b^2 + c_1(a;N)b + c_0(a;N) = 0, \tag{2.18}$$

where

$$c_2(a;N) = \frac{a^2}{2N(1-a^{2N})^3}[(N-1) - 2Na^2 + (2N^2 - 2N + 2)a^{2N} - 2N(N-1)a^{2N+2} + (N-1)a^{4N}], \tag{2.19}$$

$$c_1(a;N) = \frac{a^2}{2N(1-a^{2N})^2}[(3N-1) - 4Na^2 + (2N^2 - 4N + 2)a^{2N} - 2N(N-2)a^{2N+2} + (N-1)a^{4N}], \tag{2.20}$$

$$c_0(a;N) = -a^4 + a^2, \tag{2.21}$$

so that the solution for $b(a;N)$ can be given explicitly as

$$b(a;N) = \frac{-c_1(a;N) + \sqrt{[c_1(a;N)]^2 - 4c_2(a;N)c_0(a;N)}}{2c_2(a;N)}. \tag{2.22}$$

The second solution of the quadratic (2.18) is found not to give rise to a univalent conformal mapping for any choice of a or N and is therefore physically inadmissible. It is also noted that, throughout the range of existence of solutions, the discriminant $[c_1(a,N)]^2 - 4c_2(a,N)c_0(a,N)$ never vanishes.

In the neighbourhood of z_a, the most singular term in the velocity field is

$$u - \mathrm{i}v = -\frac{\mathrm{i}b\omega R z_\zeta(a^{-1})}{2Na^2}\frac{1}{z - z_a} + O(1), \tag{2.23}$$

so that the strength Γ_s of the satellite line vortices is given by the formula

$$\Gamma_s = -\frac{\pi b\omega R z_\zeta(a^{-1})}{Na^2}. \tag{2.24}$$

This quantity is purely real, as required.

The normalization parameter R is arbitrary. Here, it is chosen so that the satellite line vortices are unit distance from the origin for all values of a and N. This implies that

$$R(a;N) = \left(a + \frac{ba}{1-a^{2N}}\right)^{-1}. \tag{2.25}$$

With this normalization, the area of the central vortex patch, and therefore its total circulation, change with a. Let $\mathscr{A}(a;N)$ denote the area of the patch with parameter choices a and N. The circulation of the central vortex patch (denoted Γ_p) is then

$$\Gamma_p = \omega\mathscr{A}(a;N). \tag{2.26}$$

2.2. *Non-existence of solutions for* $N = 2$

It remains for us to examine whether, for any given N and a, condition (2.17) can be solved for b such that (2.13) is a globally univalent conformal mapping function

N	$a_{crit}^{(N)}$
3	5.775
4	2.565
5	1.903
6	1.627
7	1.478
8	1.385
9	1.322
10	1.276
11	1.242
12	1.215

TABLE 1. $a_{crit}^{(N)}$.

from the unit ζ-circle. The case $N = 2$ is considered first in an attempt to find a tripole-like structure in which a central V-state in solid-body rotation is surrounded by two line vortex singularities. In this case, it is found that the parameters a and b do not result in a univalent mapping from the unit ζ-circle. This is a necessary condition for a physically admissible solution. Thus, tripole-like solutions within the proposed class do not seem to exist. This does not preclude the existence of solutions of the Euler equation in which a vortex patch is surrounded by two satellite line vortices – recall that, in our analysis, the solution class has been restricted to central vortex patches that are in pure solid-body rotation. Carton & Legras (1994) have considered exactly this class of model tripole solution but only investigated a set of approximate evolution equations following a theory put forward by Legras & Dritschel (1991).

2.3. *N-symmetric co-rotating arrays, $N \geqslant 3$*

Solutions within this class can be found for all integers $N \geqslant 3$. For any given N, there exists a range of a values for which (2.17) is satisfied and which yield parameter pairs (a, b) that provide univalent conformal mappings from the unit ζ-circle. This range of existence for each N is denoted

$$a \in [a_{crit}^{(N)}, \infty), \tag{2.27}$$

i.e. there exists a lower bound $a_{crit}^{(N)}$ on the parameter a for which physically admissible equilibrium solutions can be found. For $N = 3$, the value $a_{crit}^{(3)} = 5.775$ is obtained (correct to 3 decimal places). Table 1 gives values of $a_{crit}^{(N)}$ for N between $N = 3$ and $N = 12$. The range of a-values for which solutions exist increases as N increases. It is possible to find $a_{crit}^{(N)}$ by finding the equilibrium solution which also satisfies

$$z_\zeta(\exp(\pi \mathrm{i}/N)) = 0. \tag{2.28}$$

The reason for solving (2.28) is explained in the next section.

A graph of b against a for values of N between 3 and 7 is shown in figure 2. For all values of N, b is found to be a monotonic increasing function of a. An asymptotic analysis of (2.17) (or (2.18)) reveals that

$$b(a; N) \sim \frac{2Na^2}{(N-1)} \quad \text{as } a \to \infty. \tag{2.29}$$

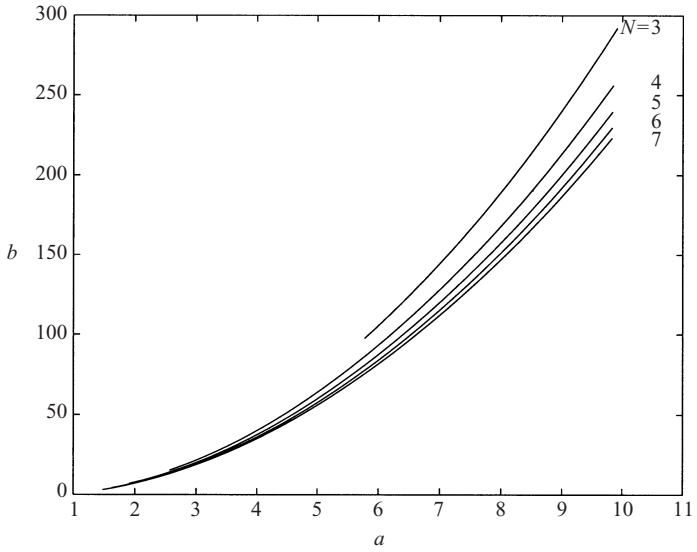

FIGURE 2. b as a function of a for $N = 3$, 4, 5, 6 and 7.

It can be shown that

$$\mathscr{A}(a;N) \sim \frac{\pi}{a^2} \quad \text{as } a \to \infty, \tag{2.30}$$

so that the central patch vanishes in the limit $a \to \infty$, resulting in a co-rotating configuration of N line vortices equally spaced around the unit circle, as considered in the classic work of Thomson (1882). Equation (2.29) can be used in (2.13) to show

$$z(\zeta) \sim \frac{1}{a\zeta} \quad \text{as } a \to \infty, \tag{2.31}$$

which implies that, for large but finite a, the central vortex patch is small and almost circular. Physically, this limit corresponds to a small near-circular Rankine vortex being placed in the stationary point flow at the centre of the N-polygonal configuration of co-rotating line vortices considered by Thomson (1882).

Because ω is arbitrary, the dynamically important quantity is the ratio of the total circulation of the central patch to the circulation of the satellite line vortices, i.e. Γ_p/Γ_s. Figure 3 shows graphs of this ratio as a function of a for N between 3 and 7 while figure 4 shows the same graph for N between 8 and 12. For a large, this ratio tends to zero because, by (2.26) and (2.30), the central patch circulation Γ_p vanishes in this limit. For $N = 3$, figure 3 shows that the satellite line vortex circulation is always significantly larger than the circulation of the central patch, even for lower values of a. This disparity in circulations decreases with a for all values of N. Moreover, for higher N values, the circulations of the central patch and the satellites become commensurate and, when $N \geqslant 6$, for small enough a-values the circulation of the central patch eventually exceeds that of the satellites.

Figure 5 shows a typical streamline plot for the case $N = 3$ in the co-rotating frame. These streamline plots have many qualitative features in common with the streamline plots for a co-rotating configuration of line vortices, as plotted by Dritschel (1985); particularly noticeable in figure 5 are what Dritschel referred to as 'umbrella' regions; these are closed recirculation regions which exist as a consequence of the fact that the streamlines are being viewed from a co-rotating frame of reference. The central

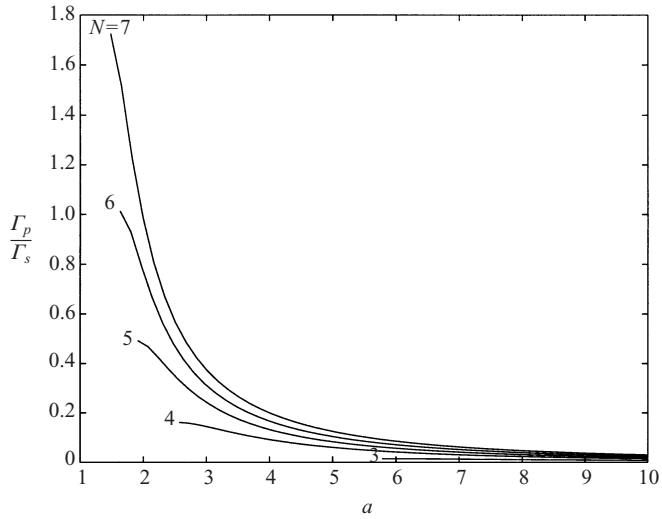

FIGURE 3. Ratio Γ_p/Γ_s as a function of a for $N = 3, \ldots, 7$.

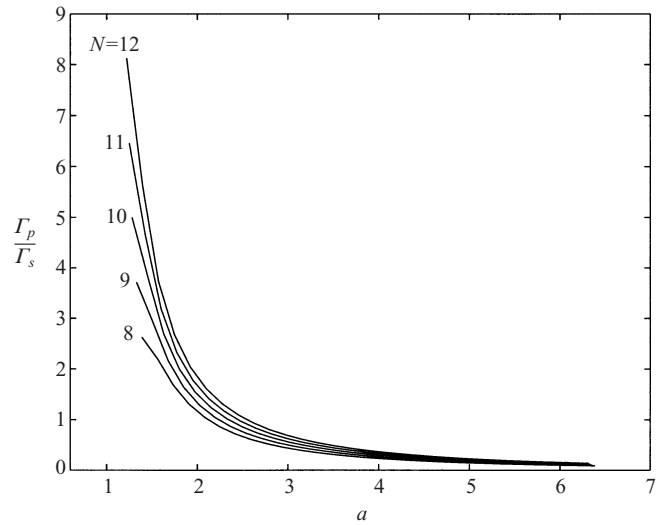

FIGURE 4. Ratio Γ_p/Γ_s as a function of a for $N = 8, \ldots, 12$.

region in which no streamlines are plotted corresponds exactly to the central vortex patch. Recall that, in a co-rotating frame, because this patch is supposed to be in solid-body rotation, the velocity field inside this patch vanishes identically. Figure 6 shows a typical streamline pattern for $N = 4$.

2.4. *Limiting patch shapes, $a \to a_{crit}^{(N)}$*

As a draws close to the lower limit of the range of existence, N zeros of z_ζ simultaneously draw close to the unit circle. For $a > a_{crit}^{(N)}$ these zeros are strictly outside the unit circle. However, when $a = a_{crit}^{(N)}$, these N zeros hit the unit circle simultaneously. One such zero is found to have argument $\pi i/N$ (by symmetry of the mapping, the remaining $N - 1$ zeros are at symmetrically disposed points about the origin). This

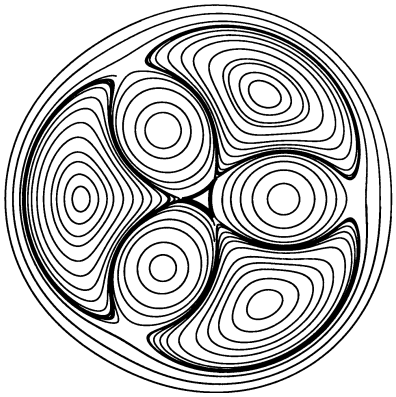

FIGURE 5. Streamlines for $N = 3$ and $a = 5.8$.

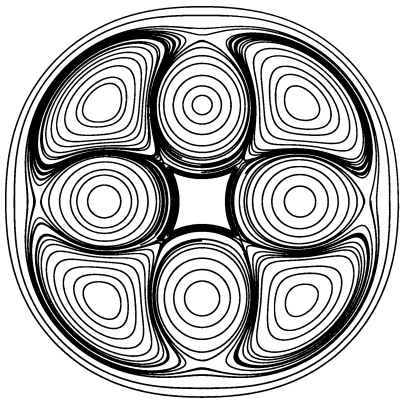

FIGURE 6. Streamlines for $N = 4$ and $a = 2.8$.

explains the reason for solving (2.28) when finding the value of $a_{crit}^{(N)}$ for any given N. It can be shown using the mapping (2.13) that (2.28) implies the following relation between b and a:

$$b = \frac{(1 + a^N)^2}{Na^N - a^N - 1}, \tag{2.32}$$

but b is also related to a and N by (2.22) so that the values $a_{crit}^{(N)}$ (table 1) are the solutions of the nonlinear equation

$$\frac{(1 + a^N)^2}{Na^N - a^N - 1} = \frac{-c_1(a;N) + \sqrt{[c_1(a;N)]^2 - 4c_2(a;N)c_0(a;N)}}{2c_2(a;N)}. \tag{2.33}$$

A zero of z_ζ reaching the unit circle corresponds to the formation of a cusp in the patch boundary. A demonstration of this is given below. The shapes of the limiting central patches are depicted in figure 7 for $N = 3$, 4 and 5.

Strictly speaking, the Schwarz function $S(z)$ used to define the velocity field (2.7) does not exist when $a = a_{crit}^{(N)}$ because the boundary ∂D ceases to be an analytic curve at this value of a. By definition, the Schwarz function $S(z)$ must be analytic in an enclosing neighbourhood of the curve ∂D and, as a result, must have a local Taylor expansion (in z) about any point on ∂D. However, when $a = a_{crit}^{(N)}$, this fails to be true. Nevertheless, this does not represent a genuine obstruction to the validity

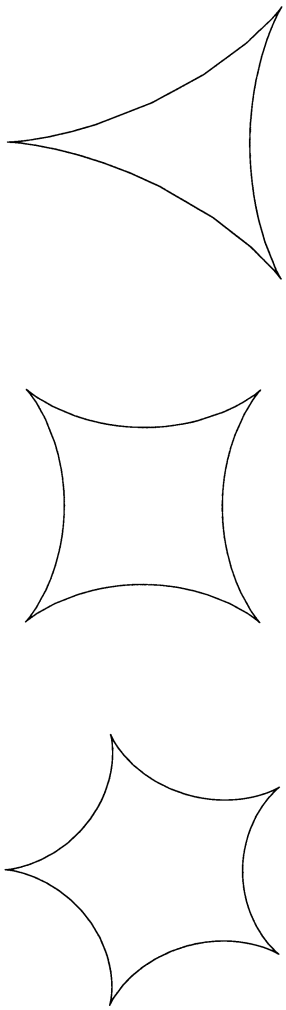

FIGURE 7. Limiting patches (or 'V-States') for $N = 3,4$ and 5; $a^{(3)}_{crit} = 5.775$, $a^{(4)}_{crit} = 2.565$, $a^{(5)}_{crit} = 1.903$.

of our solutions in the limiting case for while the function $S(z)$ can no longer be identified with the Schwarz function of the curve (when $a = a^{(N)}_{crit}$), we can still define the velocity field via equation (2.7) with $S(z)$ (no longer a Schwarz function in the strict sense) defined by (2.15). To illustrate the nature of the limiting solution in more detail, the local form of both the patch boundary shape and the velocity field in the neighbourhood of the cusp in the limiting case is now examined.

Consider the case $N = 4$ (all other N can be treated similarly). Let $a = a^{(N)}_{crit}$ and let z_c be the position of a cusp in the boundary ∂D where z_c is the image of the point $\zeta = \omega_4 = \exp(\frac{1}{4}\mathrm{i}\pi)$, i.e.

$$z_c = z_0(\omega_4). \tag{2.34}$$

z_c is on the ray $\arg[z] = -\frac{1}{4}\pi$. There are three other symmetrically disposed cusps in the patch boundary, but it is enough to consider the one at z_c. The appearance of the cusp corresponds to

$$z_{0\zeta}(\omega_4) = 0. \tag{2.35}$$

Note that when $a = a_{crit}^{(4)}$ the corresponding solution $b = b_{crit}^{(4)}$ of (2.28) is finite and well-defined (see figure 2). Indeed, we obtain

$$a_{crit}^{(4)} = 2.565, \qquad b_{crit}^{(4)} = 15.218. \tag{2.36}$$

The conformal map $z(\zeta)$ is therefore an analytic function of ζ at $\zeta = \omega_4$ and can thus be Taylor expanded as

$$z = z_c + (\zeta - \omega_4)^2 \frac{z_{0\zeta\zeta}(\omega_4)}{2!} + (\zeta - \omega_4)^3 \frac{z_{0\zeta\zeta\zeta}(\omega_4)}{3!} + \cdots, \tag{2.37}$$

where we have used (2.35). A numerical calculation reveals that $z_{0\zeta\zeta}(\omega_4) = -11.969\omega_4$ and $z_{0\zeta\zeta\zeta}(\omega_4) = -33.733$. This implies that in the vicinity of the cusp,

$$z - z_c = \alpha\omega_4(\zeta - \omega_4)^2 + \beta(\zeta - \omega_4)^3 + \cdots, \tag{2.38}$$

where $\alpha = -5.985$ and $\beta = -5.622$ are real. Alternatively, (2.38) can be written

$$(z - z_c)\omega_4 = -\alpha(\zeta\bar{\omega}_4 - 1)^2 - \beta(\zeta\bar{\omega}_4 - 1)^3 + \cdots. \tag{2.39}$$

Defining $X + \mathrm{i}Y \equiv (z - z_c)\omega_4$ (which is equivalent to mapping the position of the cusp to the origin and rotating it by $\frac{1}{4}\pi$) and letting $\zeta\bar{\omega}_4 = \exp(\mathrm{i}\phi)$ for $|\phi| \ll 1$ (which amounts to a rotation of the parametric ζ-plane by $-\frac{1}{4}\pi$ so that $\phi = 0$ corresponds to the pre-image of the cusp) then for small (real) ϕ,

$$X + \mathrm{i}Y = \alpha\phi^2 + \mathrm{i}\alpha\phi^3 + \mathrm{i}\beta\phi^3 + \cdots, \tag{2.40}$$

so that a local parametric representation of ∂D is given by

$$X = \alpha\phi^2; Y = (\alpha + \beta)\phi^3, \tag{2.41}$$

or, eliminating ϕ,

$$Y = \pm(\alpha + \beta)\left(\frac{X}{\alpha}\right)^{3/2}, \tag{2.42}$$

which, because $\alpha < 0$, has real solutions for Y when $X < 0$ and represents a $\frac{3}{2}$-cusp at $X = Y = 0$, symmetric about the x-axis.

We now find the local form of the associated velocity field. As a function of ζ, $S(z(\zeta))$, as defined by (2.15), is similarly analytic at $\zeta = \omega_4$ and, as a result, also has a Taylor expansion about this point. Indeed, defining $\mathscr{S}(\zeta)$ as

$$\mathscr{S}(\zeta) \equiv S(z(\zeta)), \tag{2.43}$$

we have

$$\mathscr{S}(\zeta) = \mathscr{S}(\omega_4) + (\zeta - \omega_4)\mathscr{S}_\zeta(\omega_4) + (\zeta - \omega_4)^2 \frac{\mathscr{S}_{\zeta\zeta}(\omega_4)}{2!} + (\zeta - \omega_4)^3 \frac{\mathscr{S}_{\zeta\zeta\zeta}(\omega_4)}{3!} + \cdots, \tag{2.44}$$

where

$$\mathscr{S}(\omega_4) = \bar{z}_c, \quad \mathscr{S}_\zeta(\omega_4) = 0, \quad \mathscr{S}_{\zeta\zeta}(\omega_4) = -\overline{z_{0\zeta\zeta}(\omega_4)},$$
$$\mathscr{S}_{\zeta\zeta\zeta}(\omega_4) = \overline{6\omega_4 z_{0\zeta\zeta}(\omega_4) + \mathrm{i}z_{0\zeta\zeta\zeta}(\omega_4)}. \tag{2.45}$$

Equation (2.37) can be used to show that

$$(\zeta - \omega_4) = \left(\frac{2(z - z_c)}{z_{0\zeta\zeta}(\omega_4)}\right)^{1/2}\left[1 - \frac{z_{0\zeta\zeta\zeta}(\omega_4)}{6z_{0\zeta\zeta}(\omega_4)}\left(\frac{2(z - z_c)}{z_{0\zeta\zeta}(\omega_4)}\right)^{1/2} + \cdots\right], \tag{2.46}$$

so that, using (2.46) and (2.45) in (2.44), $S(z)$ is seen to have a local expansion of the form

$$S(z) = \bar{z}_c + \mathrm{i}(z - z_c) + \frac{1}{6}\left(\frac{2(z - z_c)}{z_{0\zeta\zeta}(\omega_4)}\right)^{3/2}[S_{\zeta\zeta\zeta}(\omega_4) - \mathrm{i}z_{0\zeta\zeta\zeta}(\omega_4)] + \cdots. \tag{2.47}$$

Thus, although $S(z)$ ceases to have a Taylor expansion at z_c, it has a local expansion in increasing powers of $(z - z_c)^{1/2}$. The local velocity field near the cusp z_c thus has an expansion of the form

$$u - \mathrm{i}v = \tfrac{1}{2}\mathrm{i}\omega\left((\bar{z} - \bar{z}_c) - \mathrm{i}(z - z_c) - 0.725\mathrm{i}\left(\frac{2(z - z_c)}{z_{0\zeta\zeta}(\omega_4)}\right)^{3/2} + o((z - z_c)^{3/2})\right), \tag{2.48}$$

where the third non-zero coefficient has been computed numerically. Note that the velocity field is finite at the cusp (indeed it vanishes, as it must, for continuity with the velocity field inside the patch) and no physical quantities become singular at the limiting state. Overman (1986) emphasizes that limiting V-states need not be *singular* V-states and, indeed, those found here are not.

In the case of an isolated rotating uniform vortex patch in the absence of external straining flows, it is known (Overman 1986; Saffman 1992) that the limiting states develop corners in which the tangent angle changes discontinuously by 90°. This class of rotating patches has been seen to have limiting states with cusp singularities. Overman (1986) has shown that these are the only two allowable possibilities for limiting V-states in which the tangent angle is discontinuous. He also reports that no limiting V-states exhibiting cusp singularities are known to him (although he does not rule out the possibility that they might exist). The only other solutions known to the present author in which a uniform patch of vorticity develops a cusp singularity is in a class of non-rotating hypotrochoidal vortex patch equilibria situated in a rotational polynomial straining flow which is singular at infinity. These solutions were found by Burbea (1982). The solutions found above are different from Burbea's and involve rotating V-states in which the flow vanishes at infinity. Nevertheless, in the solutions above, the central vortex patch finds itself situated in the straining flow owing to the polygonal array of surrounding line vortices and this is apparently crucial in rendering the limiting states cuspidal, rather than corner-like, in nature. This evidence suggests there is no physical reason why cuspidal limiting states in V-state equilbria cannot be realized; rather, it suggests that a vortex patch in equilibrium will only display cuspidal limiting states provided there is some (sufficiently strong) external straining mechanism (or 'forcing') on it. The self-induced flow of an isolated simply connected uniform vortex patch in equilibrium is, it seems, not strong enough to induce such a cusp.

2.5. *Limit* $N \to \infty$

Another limit of interest is $N \to \infty$. In figure 8, a typical streamline plot for $N = 25$ and $a = 1.5$ is shown and displays a distinctive 'cat's-eye' pattern developing in a radial layer at some distance outside the central vortex patch. The central vortex patch has become very nearly circular in shape. This behaviour is found to be generic: in the limit $N \to \infty$ for fixed a, an increasing number of line vortex singularities collect in an almost circular configuration some distance outside the central patch. As $N \to \infty$, this collection of line vortex singularities draws close to the singular limit of a uniform vortex sheet (Saffman 1992) surrounding the central vortical patch. Moreover, provided this vortex-sheet structure is not too close to the central vortex

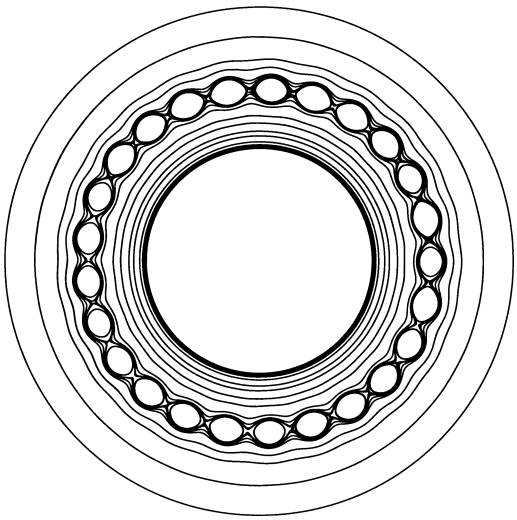

FIGURE 8. Streamlines for $N = 25$ and $a = 1.5$. As $N \to \infty$ the collection of satellite line vortices tends to form a circular vortex sheet of uniform strength surrounding the central patch.

patch, the central patch becomes indistinguishably close to a circle. In the limit $N \to \infty$, a typical solution tends to a circular vortex sheet surrounding a uniform circular vortex patch.

To see this, note that as $N \to \infty$ for fixed $a > 1$ (for which solutions exist) it can be shown that

$$c_0 \sim a^2 - a^4, \qquad c_1 \sim \frac{a^2}{2}, \qquad c_2 \sim -\frac{a^2}{2}\frac{1}{a^{2N}}, \tag{2.49}$$

so that c_2 becomes exponentially small while c_0 and c_1 tend to finite limits. It is straightforward to show that, in the same limit,

$$b \sim 2(a^2 - 1). \tag{2.50}$$

Using (2.50) in (2.25) implies that

$$R \sim \frac{1}{a}. \tag{2.51}$$

Using all this information in the conformal map (2.13) implies that, for ζ on the unit-ζ circle,

$$z(\zeta) = R\left(\frac{1}{\zeta} + \frac{b\zeta^{N-1}}{\zeta^N - a^N}\right) \sim \frac{1}{a\zeta}\left(1 - \frac{2(a^2-1)}{a^N}\zeta^N\right). \tag{2.52}$$

Equation (2.52) shows that the patch tends to a circular disk, of radius $1/a$, with small (in fact exponentially small, in the limit) N-fold symmetric ripples on its boundary.

It is also found that $a_{crit}^{(N)}$ tends to unity for large N (this can be established by a large-N analysis of the solutions to (2.33), the details are omitted here). From (2.52) this implies that for large N and a close to $a_{crit}^{(N)}$, the central vortex patch is very close to the circular band of cat's eyes. In the double limit, $N \to \infty$ and $a \to a_{crit}^{(N)}$, it is expected that the solution will tend to the configuration in which a Rankine vortex (Saffman 1992) has a circular vortex sheet of uniform strength at its boundary.

3. Linear stability analysis

The linear stability of the exact solution class is now studied. Under a general irrotational perturbation, using Helmholtz laws, the velocity field in the co-rotating frame can be written

$$u - \mathrm{i}v = \begin{cases} -\frac{1}{2}\mathrm{i}\omega G(z,t), & z \in D(t), \\ \frac{1}{2}\mathrm{i}\omega\left(\bar{z} - \sum_{k=1}^{N} \dfrac{\gamma_s}{z - z_k(t)} - F(z,t)\right), & z \notin D(t), \end{cases} \tag{3.1}$$

where $G(z,t)$ is analytic inside $D(t)$ and $F(z,t)$ analytic outside $D(t)$ and is $O(1/z)$ as $|z| \to \infty$. Continuity of velocity on the vortex jump requires that

$$G(z,t) - F(z,t) = -\bar{z} + \sum_{k=1}^{N} \frac{\gamma_s}{z - z_k(t)} \quad \text{on } \partial D(t). \tag{3.2}$$

Equation (3.2) is a scalar Riemann–Hilbert problem. The solution for $F(z,t)$, decaying as $|z| \to \infty$, is given by the Cauchy integral

$$F(z,t) = \frac{1}{2\pi\mathrm{i}} \oint_{\partial D(t)} \left(-\bar{z}' + \sum_{k=1}^{N} \frac{\gamma_s}{z' - z_k(t)}\right) \frac{\mathrm{d}z'}{z' - z} = -\frac{1}{2\pi\mathrm{i}} \oint_{\partial D(t)} \frac{\bar{z}'\,\mathrm{d}z'}{z' - z}, \quad z \notin D(t), \tag{3.3}$$

the second equality following because the points $\{z_k(t)\}$ are outside $D(t)$. The perturbation to the base state conformal map (hereinafter, denoted $z_0(\zeta)$) is given by

$$z(\zeta,t) = z_0(\zeta) + \epsilon \exp(\sigma t)\hat{z}(\zeta), \tag{3.4}$$

and the perturbed positions of the line vortices given by

$$z_k(t) = z_{k0} + \epsilon \exp(\sigma t)\hat{z}_k, \quad k = 1, \ldots, N, \tag{3.5}$$

where $\epsilon \ll 1$ is a small parameter and where $\hat{z}(\zeta)$, $\hat{z}_k$ and σ are to be determined. z_{k0} denote the equilibrium positions of the line vortices as found in § 2.

To find the linear stability spectrum, a spectral method based on Taylor and Laurent expansions is used. The function $\zeta\hat{z}(\zeta)$ has a Taylor expansion of the form

$$\zeta\hat{z}(\zeta) = \sum_{n=0}^{\infty} \hat{a}_n \zeta^n, \tag{3.6}$$

and its conjugate function has an expansion of the form

$$\zeta^{-1}\bar{\hat{z}}(\zeta^{-1}) = \sum_{n=0}^{\infty} \frac{\hat{a}_n^*}{\zeta^n}, \tag{3.7}$$

where it is assumed that the sets $\{a_n\}$ and $\{a_n^*\}$ are independent quantities. For numerical computation, the expansions (3.6) and (3.7) are truncated at order $\frac{1}{2}\mathcal{N} - 1$ where $\mathcal{N}$ is an even integer.

If ζ_{k0} denote the pre-images in the ζ-plane of the points z_{k0}, the quantities $\{\hat{\zeta}_k | k = 1, \ldots, N\}$ are defined via the equations

$$z_k(t) = z_{k0} + \epsilon \exp(\sigma t)\hat{z}_k \equiv z(\zeta_{k0} + \epsilon\hat{\zeta}_k, t), \quad k = 1, \ldots, N, \tag{3.8}$$

so that, to leading order in ϵ,

$$\hat{z}_k = \hat{\zeta}_k z_{0\zeta}(\zeta_{k0}) + \hat{z}(\zeta_{k0}), \quad k = 1, \ldots, N. \tag{3.9}$$

Similarly,

$$\overline{\hat{z}_k} = \hat{\zeta}_k^* z_{0\zeta}(\bar{\zeta}_{k0}) + \overline{\hat{z}(\zeta_{k0})}, \quad k = 1, \ldots, N. \tag{3.10}$$

The set $\{\hat{\zeta}_k^* \,|\, k = 1, \ldots, N\}$ is assumed to be independent of the set $\{\hat{\zeta}_k \,|\, k = 1, \ldots, N\}$.

After truncation, the set of unknowns is as follows:

$$\{\hat{a}_k \,|\, k = 0 \ldots \tfrac{1}{2}\mathcal{N} - 1\}, \quad \{\hat{a}_k^* \,|\, k = 0 \ldots \tfrac{1}{2}\mathcal{N} - 1\},$$
$$\{\hat{\zeta}_k |\ k = 1, \ldots, N\}, \quad \{\hat{\zeta}_k^* |\ k = 1, \ldots, N\}. \tag{3.11}$$

This constitutes a set of $\mathcal{N} + 2N$ unknowns. To eliminate a rotational degree of freedom associated with the Riemann mapping theorem, the condition

$$a_0 = a_0^*, \tag{3.12}$$

is imposed. This reduces the total number of unknowns to $\mathcal{N} - 1 + 2N$.

By composition of analytic functions, we can define $\mathscr{F}_0(\zeta)$ via

$$\mathscr{F}_0(\zeta) \equiv F_0(z_0(\zeta)), \tag{3.13}$$

and similarly $\hat{\mathscr{F}}(\zeta)$ via

$$F(z(\zeta, t), t) = \mathscr{F}_0(\zeta) + \epsilon \hat{\mathscr{F}}(\zeta) \exp(\sigma t) + O(\epsilon^2). \tag{3.14}$$

To find $\hat{\mathscr{F}}(\zeta)$, first note that because $F(z, t)$ is analytic outside D then it has a Laurent series of the form

$$F(z, t) = \sum_{k=0}^{\infty} \frac{F_k}{z^{k+1}}. \tag{3.15}$$

It can be shown from (3.3) that

$$F_k \equiv \frac{1}{2\pi \mathrm{i}} \oint_{\partial D} \bar{z}' z'^k \, \mathrm{d}z', \quad k = 0, 1, 2, \ldots . \tag{3.16}$$

These coefficients depend on ϵ. Linearizing for small ϵ, so that,

$$F_k = F_{k0} + \epsilon \hat{F}_k \exp(\sigma t) + O(\epsilon^2), \tag{3.17}$$

it follows that

$$\hat{F}_k = -\frac{1}{2\pi \mathrm{i}} \left[\oint_{|\zeta|=1} \overline{\hat{z}}(\zeta^{-1})(z_0(\zeta))^k z_{0\zeta}(\zeta) \, \mathrm{d}\zeta \right.$$
$$\left. + \oint_{|\zeta|=1} k \bar{z}_0(\zeta^{-1})(z_0(\zeta))^{(k-1)} z_{0\zeta}(\zeta) \hat{z}(\zeta) \, \mathrm{d}\zeta + \oint_{|\zeta|=1} \bar{z}_0(\zeta^{-1})(z_0(\zeta))^k \hat{z}_\zeta(\zeta) \, \mathrm{d}\zeta \right]. \tag{3.18}$$

The linearized kinematic boundary condition provides some of the $\mathcal{N} - 1 + 2N$ equations required to find the $\mathcal{N} - 1 + 2N$ unknowns. Some algebraic manipulation reduces the linearized kinematic boundary condition to

$$\sigma \mathrm{Re}\left[\frac{\bar{z}_{0\zeta}(\zeta^{-1}) \hat{z}(\zeta)}{\zeta} \right] = \mathrm{Re}\left[-\tfrac{1}{2} \mathrm{i} \omega \zeta z_{0\zeta} \left(\sum_{j=1}^{N} \frac{\gamma_s \hat{z}_j}{(z_0(\zeta) - z_{j0})^2} + \sum_{k=0}^{\infty} \frac{\hat{F}_k}{(z_0(\zeta))^{(k+1)}} \right) \right]. \tag{3.19}$$

Equations (3.6), (3.7) (3.9) and (3.10) are substituted into (3.19) and the equation expanded as a Laurent series. Equating coefficients on both sides of (3.19) for ζ between $\zeta^{-(\mathcal{N}/2)+1}$ and $\zeta^{(\mathcal{N}/2)-1}$, provides $\mathcal{N} - 1$ equations. The infinite sum appearing in (3.19) is truncated, consistently, after the $k = \frac{1}{2}\mathcal{N} - 1$ term.

The linearized equations for the line vortices provide the remaining $2N$ equations. These are given by

$$\sigma\overline{\hat{z}_k} = \tfrac{1}{2}\mathrm{i}\omega\left(\overline{\hat{z}_k} - \sum_{j\neq k}\frac{\gamma_s(\hat{z}_j - \hat{z}_k)}{(z_{k0}-z_{j0})^2} - \hat{F}_k^{(lv)}\right), \quad k = 1,\ldots,N, \tag{3.20}$$

and its complex conjugate, where

$$\hat{F}_k^{(lv)} = \frac{1}{2\pi\mathrm{i}}\oint_{|\zeta|=1}\frac{\overline{\hat{z}}(\zeta^{-1})z_{0\zeta}(\zeta)}{z_0(\zeta)-z_{k0}}\,\mathrm{d}\zeta + \frac{1}{2\pi\mathrm{i}}\oint_{|\zeta|=1}\frac{\overline{z}_0(\zeta^{-1})\hat{z}_\zeta(\zeta)}{z_0(\zeta)-z_{k0}}\,\mathrm{d}\zeta$$
$$+\frac{1}{2\pi\mathrm{i}}\oint_{|\zeta|=1}\frac{\overline{z}_0(\zeta^{-1})z_{0\zeta}(\zeta)(\hat{z}_k-\hat{z}(\zeta))}{(z_0(\zeta)-z_{k0})^2}\,\mathrm{d}\zeta, \tag{3.21}$$

To solve the system, the set (3.11) is vectorized to produce a vector $\boldsymbol{x}$ to be determined. The $\mathscr{N}-1+2N$ equations above lead to a generalized eigenvalue problem of the form

$$\boldsymbol{A}\boldsymbol{x} = \sigma\boldsymbol{B}\boldsymbol{x}, \tag{3.22}$$

where the matrices $\boldsymbol{A}$ and $\boldsymbol{B}$ depend on the base state equilibrium. For convenience, all Taylor/Laurent coefficients of functions of the base-state conformal map (and its derivatives and integrals) are computed by evaluating these functions at $\mathscr{M}$ points on the unit ζ-circle and using fast Fourier transforms. To avoid unacceptable aliasing errors, we take $\mathscr{M} \geqslant 4\mathscr{N}$. Most of the results which follow use $\mathscr{N} = 64$ and $\mathscr{M} = 256$.

3.1. *Checks of the linear stability analysis*

It is known that the dynamics of point vortices and patches of uniform vorticity is Hamiltonian (Saffman 1992). Therefore, any eigenvalues that do not occur as pure-real or pure-imaginary pairs will occur in complex conjugate quartets. This provides a simple first check on the numerical code.

Only perturbations which preserve the patch area and the vortex centroid are of interest in assessing the linear stability of the configurations. For any steady state, there exists a neighbouring equilibrium corresponding to a different value of R, i.e. an equilibrium in which the rotating patch has a slightly different area. For any a and N, we therefore expect to find a zero eigenvalue corresponding to these neighbouring steady solutions of different area. This is found to be the case. This mode is recognized and discarded – only perturbations which preserve the area of the vortex patch and vortex centroid are considered in assessing the linear stability. The fact that the patch area, vortex centroid and total angular momentum are linearly conserved quantities is used as a check on the accuracy of the calculation of the general eigenvectors.

As $a \to \infty$, the configurations tend to a situation in which a small, near-circular Rankine vortex is placed in the stationary point flow due to a configuration of N co-rotating satellite vortices as considered by Thomson (1882). Thus, as $a \to \infty$, we expect that the linear stability spectrum will tend to a direct sum of the eigenvalues associated with the shape modes of an isolated circular Rankine vortex (which, in a co-rotating frame of reference, are all given by $\sigma = \frac{1}{2}\mathrm{i}\omega$) and the finite set of eigenvalues associated with a co-rotating circular array of N satellite vortices each of strength Γ_s. The latter linear stability problem is classical (Thomson 1882; Havelock

1931; Saffman 1992) and is given, in our notation, by

$$\sigma = \pm\tfrac{1}{4}\omega\gamma_s\sqrt{k(N-k)(k(N-k)-2(N-1))}, \quad k = 0, 1, \ldots, (N-1). \tag{3.23}$$

As $a \to \infty$, the numerical method retrieves these values to spectral accuracy.

A note on a limitation of the numerical method. The method used relies on Laurent expansions of the function $F(z)$. As $a \to a_{crit}^{(N)}$ it must be expected that the numerical method will become increasingly inaccurate for fixed values of $\mathscr{N}$ and $\mathscr{M}$ as a result of attempting to evaluate an expansion at radii too close to its radius of convergence (this is intimately related to the fact demonstrated earlier that in the limit $a \to a_{crit}^{(N)}$ the function $S(z)$, and hence $F(z)$, fails to be analytic in an enclosing neighbourhood of ∂D). Indeed, for a-values sufficiently far from $a_{crit}^{(N)}$ it is found that independently increasing $\mathscr{N}$ and $\mathscr{M}$ do not affect the results of the eigenvalue calculation; however, if a is too close to $a_{crit}^{(N)}$ it is found that the spectrum is susceptible to significant changes as the order of the method is increased. This means that using the method above, we cannot compute the linear stability of solutions with values of a too close to $a_{crit}^{(N)}$.

3.2. *Results*

It is well-known (Thomson 1882; Saffman 1992) that a circular array of N co-rotating vortices (with no central line vortex) is a linearly stable configuration for $2 \leqslant N < 7$, is neutrally stable for $N = 7$ and unstable for $N > 7$. In the limit $a \to \infty$, the central vortex patch vanishes leaving precisely such a co-rotating system of line vortices. Morikawa & Swenson (1971) have studied the case of a central line vortex placed at the centre of a co-rotating configuration of unit-strength line vortices and found that, if the circulation of the central line vortex is less than unity, the equilibria are stable for $N = 3$, 4, 5, 6 and 7. See table 1 of Morikawa & Swenson (1971). It is therefore expected that, at least for large a, cases $N = 3$, 4, 5, 6 and possibly $N = 7$ are reasonable candidates for being linearly stable configurations. Morikawa & Swenson (1971) also find that a central line vortex of sufficiently strong positive vorticity eventually stabilizes the total N-polygonal line vortex configuration for any $N \geqslant 8$. For example, a central line vortex of strength greater than 0.5, but less than 12.25, sitting at the centre of eight unit-circulation line vortices represents a stable configuration. Table 1 of Morikawa & Swenson (1971) provides the stability ranges for higher values of N. Figure 4 shows that the relative circulation of the central vortex patch increases with decreasing a for $N \geqslant 8$. Therefore, although we expect the large-a configurations for $N \geqslant 8$ to be linearly unstable, *a priori* it is conceivable that the configurations could stabilize at smaller values of a.

The results of the calculation show that for N between 3 and 7 inclusive, the configurations are linearly stable for the entire range of a-values that could be reliably analysed using the numerical method described above. No eigenvalues with positive real part are found (for $N = 3, 4, \ldots, 7$) for any a value that is not too close to $a_{crit}^{(N)}$ (typically, only when a is within approximately 0.1 of $a_{crit}^{(N)}$ do the results of the numerical method become unreliable. This manifests itself by large changes in the computed spectrum as the order of the method is increased). Note that, in respect of the solutions for non-rotating patches in an infinite polynomial straining flow computed by Burbea (1982), the author states (without including details) that the entire class of patches is stable except for the limiting cuspidal state. The present author can find no further corroboration of this statement in the literature. It is possible that a similar situation holds for the class of rotating solutions found here

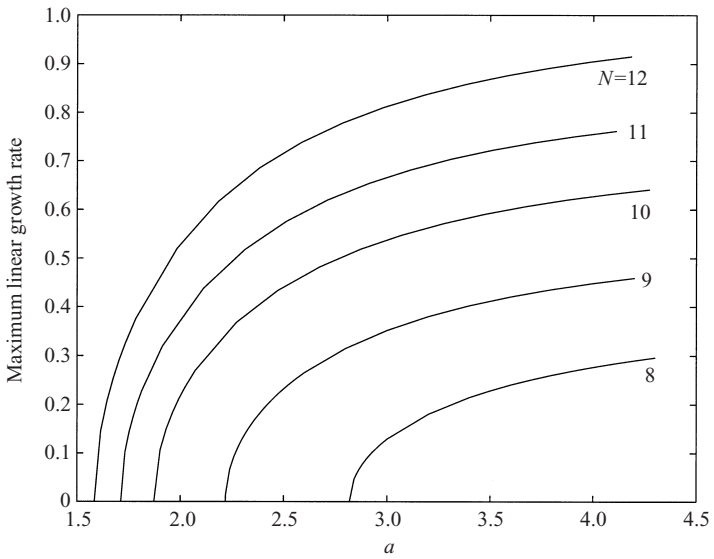

FIGURE 9. Maximum linear growth rates against a for $N = 8, \ldots, 12$.

although we can make no definite statement about this until a method capable of accurately computing the linear stability spectrum of the close-to-limiting states is implemented.

As expected, for $N \geqslant 8$ the large-a configurations are linearly unstable. However, in the cases $N = 8$, 9, 10, 11 and 12 which have been examined in detail, there exists a critical a value at which the maximum linear growth rate becomes zero. Figure 9 shows the maximum linear growth rate plotted as a function of a for N between 8 and 12 inclusive. The critical a values at which exchange of stability occurs will be denoted $a_{stab}^{(N)}$. When $N = 8$ it is found that at $a = 2.819 = a_{stab}^{(8)}$, a $\pm$-pair of real eigenvalues (the only real eigenvalues in the spectrum) pass through zero and, for $a < 2.819$, become pure imaginary. For $N = 9$, it is found that at $a = 2.219 = a_{stab}^{(9)}$ two repeated $\pm$-pairs (the only real eigenvalues in the spectrum) similarly pass through zero and become pure imaginary for $a < 2.219$ thereby rendering the configuration linearly stable. Such behaviour is similarly found to occur for all higher values of N analysed. It is conjectured that the states are linearly stable for all values in the open interval $a \in (a_{crit}^{(N)}, a_{stab}^{(N)})$ although corroboration of this requires further investigation. For N even, a $\pm$-pair of real eigenvalues becomes pure imaginary whereas for N odd, a repeated $\pm$-pair of real eigenvalues become pure imaginary. The values of $a_{stab}^{(N)}$ are shown in table 2.

Morikawa & Swenson (1971) observe that an unstable configuration of $N \geqslant 8$ unit-circulation satellite line vortices is stabilized by a sufficiently strong positive central line vortex. The same appears to be true of the exact solutions found here when the total circulation of the central vortex patch is sufficiently large. For purposes of comparison, the value of a (for each $N \geqslant 8$) at which the ratio of the circulations of the central vortex patch and the satellite line vortices equals the critical ratio for linear stability, as calculated by Morikawa & Swenson, is calculated. For example, Morikawa & Swenson (1971) found that if the ratio of the circulation of a central line vortex to that of each of 8 satellite line vortices is greater than 0.5 then the configuration is linearly stable. The value of a at which $\Gamma_p/\Gamma_s = 0.5$ is found to be

N	$a_{stab}^{(N)}$	$a_{MS}^{(N)}$
8	2.819	2.828
9	2.219	2.235
10	1.872	1.889
11	1.712	1.731
12	1.584	1.603

TABLE 2.

N	$\dfrac{(a_{MS}^{(N)} - a_{stab}^{(N)})}{a_{stab}^{(N)}}$	$\left.\dfrac{b}{a^N}\right\vert_{a_{stab}^{(N)}}$
8	0.0032	0.0040
9	0.0072	0.0068
10	0.0091	0.010
11	0.011	0.012
12	0.012	0.013

TABLE 3.

$a = 2.828$. This value of a has been calculated for N between 8 and 12 inclusive and is denoted $a_{MS}^{(N)}$. The computed values of $a_{MS}^{(N)}$ are also shown in table 2 to facilitate comparison with the values of $a_{stab}^{(N)}$. In the cases analysed, the difference between $a_{stab}^{(N)}$ and $a_{MS}^{(N)}$ is found to be of the order of just 1%.

The following explanation for the closeness of $a_{stab}^{(N)}$ to $a_{MS}^{(N)}$ can be offered. For large values of N, it is found that the shapes of the central vortex patches when $a = a_{stab}^{(N)}$ are very close to circular. The central vortex patch can therefore be modelled, to a good approximation, by a circular Rankine vortex of the same total circulation and it is well-known that the irrotational flow field induced outside a Rankine vortex is equivalent to that induced by replacing the Rankine vortex with a point vortex of the same total circulation at its centre.

To test this idea, it is noted that for $N \geqslant 8$, the values of $(a_{stab}^{(N)})^N$ are much greater than unity, thus for ζ on the unit ζ-circle,

$$z(\zeta) = R\left(\frac{1}{\zeta} + \frac{b\zeta^{N-1}}{\zeta^N - a^N}\right) \approx \frac{R}{\zeta}\left(1 - \frac{b}{a^N}\zeta^N\right), \tag{3.24}$$

where a has the value $a_{stab}^{(N)}$ and b is the corresponding solution of (2.22). Equation (3.24) shows that the patch is a radius-R circular disk (i.e. a Rankine vortex) to within an N-fold symmetric ripple of amplitude Rb/a^N. Given this, and assuming the above explanation for the discrepancy between $a_{stab}^{(N)}$ and $a_{MS}^{(N)}$ is correct, it is reasonable to expect that the relative discrepancy $(a_{MS}^{(N)} - a_{stab}^{(N)})/a_{stab}^{(N)}$ might be of the same order as b/a^N (evaluated at $a_{stab}^{(N)}$) – the relative departure of the central patch (at the stability boundary) from a perfect Rankine vortex. This is found to be the case. Table 3 shows these values for N between 8 and 12.

The fact that $a_{stab}^{(N)} \approx a_{MS}^{(N)}$ is of practical value. Morikawa & Swenson (1971) describe a simple algorithm for computing $a_{MS}^{(N)}$ for any N. Therefore, assuming that $a_{stab}^{(N)} \approx a_{MS}^{(N)}$ for all $N \geqslant 8$, good estimates of the linear stability regions of the exact solutions

found here can thus be obtained for higher values of N without the need for the detailed numerical calculations just described.

4. Nonlinear evolution

It has been conjectured above that the close-to-limiting vortex configurations are neutrally stable for all N. Even if this is true, it is likely that the highly distorted shapes of the central patch might be susceptible to nonlinear instabilities associated with such effects as nonlinear steepening and filamentation or vortex stripping, especially as the near-cuspidal regions of the patch protrude outwards into the strain fields associated with the surrounding satellite vortices. If these strain fields are sufficiently perturbed (e.g. by perturbing the positions of the satellite vortices – see later) it is reasonable to expect that the protruding patch vorticity might be entrained away from the centre of the configuration. This idea is now tested by exposing the equilibria to a restricted class of perturbations and computing the fully nonlinear evolution. It is not the purpose of this section to present an exhaustive study of the nonlinear stability of the exact solutions.

The nonlinear evolution of the equilibria of § 2 is amenable to computation via the methods of contour dynamics originally expounded by Deem & Zabusky (1978) (see also a comprehensive review article by Pullin 1992). To do this, the contour surgery code developed by Dritschel (1988*b*) is supplemented by a finite set of differential equations governing (according to the laws of Helmholtz) the evolution of the set of line vortices. For convenience, the choice $\omega = 2$ is made so that the corresponding angular velocity is $\Omega = \frac{1}{2}\omega = 1$. Time is scaled with 2π, so that a single revolution period T of each exact solution is given by $T = 1$.

First, several runs (of the modified code) consisting purely of an N-polygonal array of co-rotating line vortices was made for various values of N. The angular velocity Ω of steady rotation is well-known to be given as

$$\Omega = \frac{\Gamma(N-1)}{4\pi r^2}, \tag{4.1}$$

where r is the radial distance of each line vortex from the origin, and Γ is the circulation of each vortex (Thomson 1882). It is checked that the modified contour dynamics algorithm reproduces a steady configuration rotating with this angular velocity.

Several runs were made using initial configurations given by the unperturbed solutions of § 2. About 150 points are used to specify the initial contour. For values of N between 3 and 7, it is found that provided a is sufficiently large, a typical initially unperturbed exact solution can persist with no visible change of form for up to ten period revolutions (the total duration of the computations). If a is close to $a_{crit}^{(N)}$ so that the central patch is distorted from circular, the solutions are often seen to develop a form of unsteadiness in the shape of the central patch. Undulations of the patch boundary, most pronounced in the vicinity of any near-cusps, are observed and are characterized by a repeated sharpening and smoothening of the near-cusps.

First, it is of interest to establish the nonlinear fate of the linearly unstable configurations. For initially unperturbed configurations with $N \geqslant 8$ and $a > a_{stab}^{(N)}$ the configuration will rotate for several period revolutions with no visible change of form. However, eventually the accumulation of numerical errors provides a seed for growth of the linearly unstable modes. Three time-frames of the evolution of a typical (linearly unstable) $N = 8$ solution is shown in figure 10 and reveals an interesting

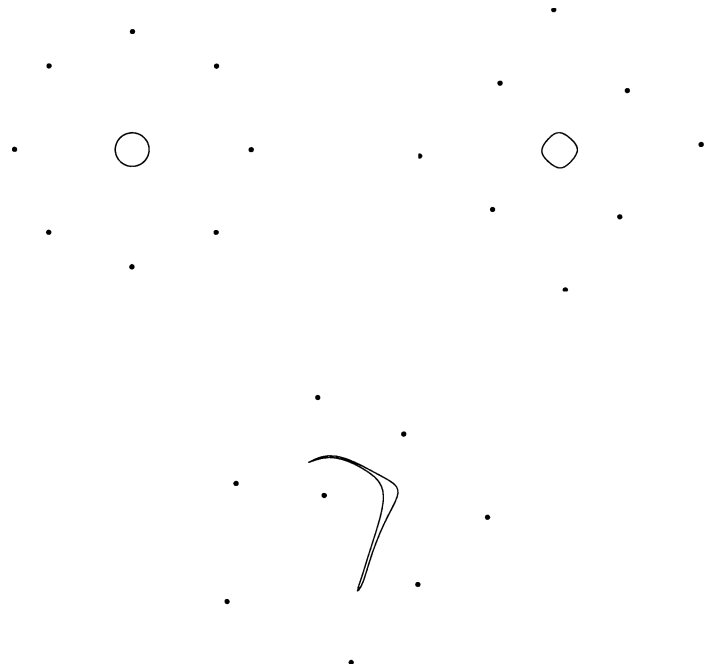

FIGURE 10. Nonlinear evolution of an initially unperturbed, linearly unstable, solution $N = 8$, $a = 7$: times $t = 0$, 3.875, 8.75. The configuration first undergoes a transition in which alternate vortices move in and out to circles on either side of the equilibrium circle before the array eventually loses all ordered structure.

feature; at time $t = 3.875$ (after nearly four period revolutions) the configuration of the 8 satellite line vortices has changed so that two distinct co-rotating rings of 4 vortices (of different radii) have formed. The same phenomenon was observed by Morikawa & Swenson (1971) (who referred to it as 'nonlinear periodic oscillations') in the case of even N and sufficiently small perturbations. By $t = 8.75$, the rotating configuration has broken down, the centroid of the central vortex patch moves away from the origin and the patch is torn apart by the effects of the strain fields induced by the satellite line vortices which have moved out of any ordered pattern. The long-time effect is a complete disintegration of the vortex array.

We now perturb the equilibria. For purposes of comparison between different a and N, consideration is restricted to a fixed perturbation type which can be sensibly defined for all choices of a and N. This is chosen to be an inward radial perturbation of $\epsilon = 0.01$ of the position of the line vortex on the positive x-axis. This is sufficiently small that it might be expected to constitute a 'linear' perturbation for most configurations, but it will also introduce asymmetric differentials in the strain field experienced by the central patch owing to the satellites. Note that this perturbation leads to an initial configuration that does not have the same angular momentum as the initial unperturbed state. Because angular momentum is conserved by the dynamics, we do not therefore expect to see the perturbed states 'relax' into the equilibria found in § 2.

Typical results are shown in figures 11–19 for $N = 3, 5$ and $N = 7$. For each N, three distinct a-values are chosen. The maximum duration of the calculations is $t = 10$. In the cases where the configuration does not survive until $t = 10$ without significant change of form, the final configurations plotted are those just before the

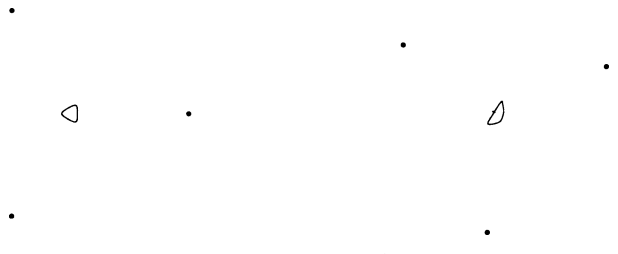

FIGURE 11. $N = 3$, $a = 15$: times $t = 0$, 10.

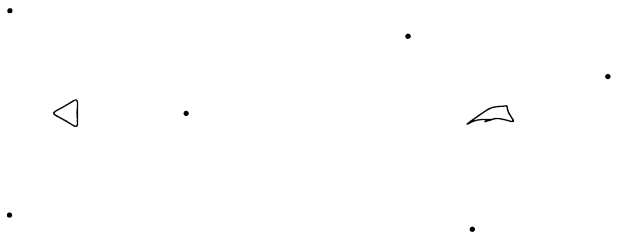

FIGURE 12. $N = 3$, $a = 10$: times $t = 0$, 2.7.

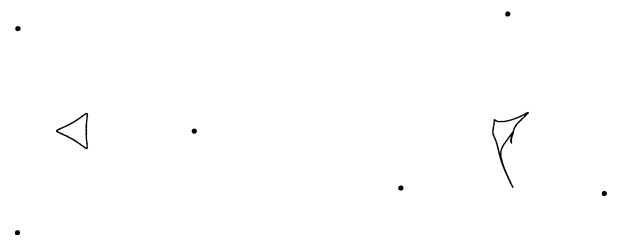

FIGURE 13. $N = 3$, $a = 8$: times $t = 0$, 1.9.

first contour surgery event. This usually occurs due to the formation of a long vortical filament protruding from the central patch.

As discussed by Morikawa & Swenson (1971), it is natural to expect that what actually constitutes a linear perturbation will itself depend on the configuration being perturbed. The case $N = 3$ appears to be unstable to the chosen perturbation even for large values of a (so that the central core is small and close to circular). Results showing distortions of the central vortex patch are shown in figures 11–13 for a descending sequence of a-values. The analysis of § 3 shows that these configurations have no linearly unstable modes. The nonlinear results suggest that the chosen perturbation is sufficiently large that it cannot be considered a linear perturbation for these configurations. A possible explanation is suggested by figure 3 which shows that, for $N = 3$, the circulation of the patch is very weak compared to the satellite line vortex circulations so that even a mild displacement of a satellite line vortex might be expected to have a significant dynamical effect on the central patch. As N increases, the central patch proves more robust to this perturbation for a larger range of a-values and maintains its overall shape for longer periods of time. As expected, for sufficiently small a (so that the central patches are quite distorted) eventually even this mild perturbation causes growth of distortions in the boundary, mainly associated with the outwardly protruding parts of the patch. The case of $N = 5$ is shown in figures 14–16. For $a = 2.0$, the entraining/stripping of the protruding parts of the central patch by the exterior straining field is clearly seen in figure 16 (this

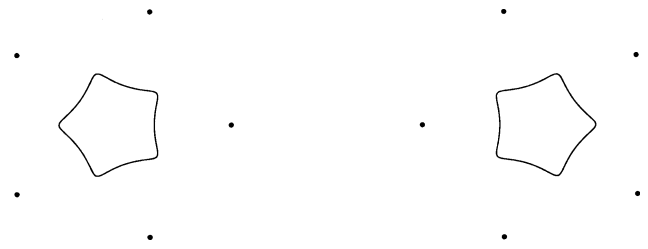

FIGURE 14. $N = 5$, $a = 2.5$: times $t = 0$, 10.

FIGURE 15. $N = 5$, $a = 2.25$: times $t = 0$, 10.

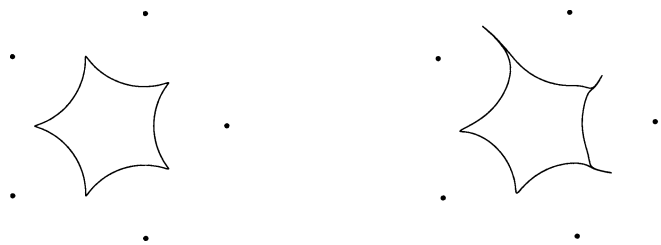

FIGURE 16. $N = 5$, $a = 2$: times $t = 0$, 1.2.

effect is also evident in figure 13 for $N = 3$). Although all the configurations in figures 14–16 have no linearly unstable modes, the nonlinear calculations suggest that the threshold on the size of perturbations which are accurately described within linear theory decreases with decreasing a for fixed N. (To test this quantitatively, a weakly nonlinear analysis would be appropriate, but is beyond the scope of the present paper.) On the other hand, as N increases, the arrays appear to become more robust to this perturbation for a wider range of a values. Figures 17–19 show calculations for $N = 7$ right up to $t = 10$ and no significant change in form in either the structure of the array or the vortex patch shape is observed. The nonlinear evolution of linearly stable configurations for $N \geqslant 8$ is found to be similar to the $N = 7$ case in figure 19.

5. Final remarks

It is useful to have knowledge of explicit solutions of the two-dimensional Euler equation. This paper has presented a wide class of explicit solutions involving regions of distributed vorticity and has analysed their linear stability properties. It has not been possible, with the method of analysis used herein, to ascertain the linear stability properties of the configurations which are close to limiting. Nevertheless, for N between 3 and 7, all configurations investigated are found to be neutrally stable. For N between 8 and 12, the configurations are neutrally stable for sufficiently small a. It

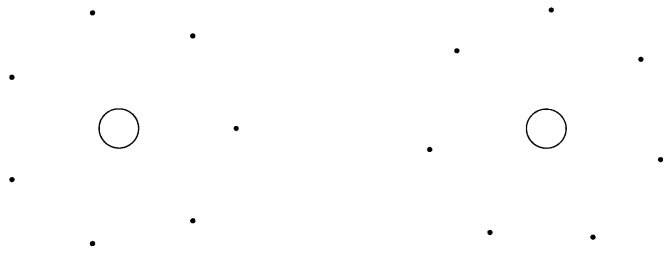

FIGURE 17. $N = 7$, $a = 6.0$: times $t = 0$, 10.

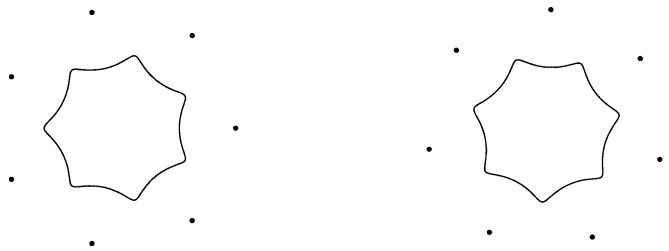

FIGURE 18. $N = 7$, $a = 2.0$: times $t = 0$, 10.

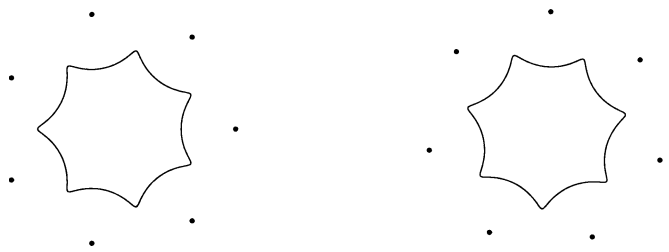

FIGURE 19. $N = 7$, $a = 1.65$: times $t = 0$, 10.

is interesting that, for N between 8 and 12, the configurations with small near-circular central patches are linearly unstable, but those with larger, geometrically non-trivial central patches prove to be stable. It is expected that solutions with $N > 12$ display similar properties.

It is convenient that the nonlinear evolution of the solution class can be studied by adapting pre-existing contour dynamics codes. Here, only limited examples of the nonlinear evolution have been studied. Including perturbations of the central patch boundaries, there are an infinite number of ways in which the solution class might be nonlinearly perturbed. In any given application of the solutions to a physical problem, the application itself will suggest which class of perturbations might be of interest.

The author wishes to thank Professors H. Aref and D. Dritschel for useful discussions during a workshop at the Newton Institute in Cambridge in December 2000. The author also thanks Professor Dritschel for explaining his contour surgery code and Martin Cloke for useful discussions. This research is partially supported by a grant from the Nuffield Foundation. The author also thanks the anonymous referees for a number of useful suggestions.

REFERENCES

Acheson, D. J. 1990 *Elementary Fluid Dynamics*. Oxford University Press.

Aref, H. A. 1998 Point vortices exhibit asymmetric equilibria. *Nature* **392**, 769.

Bauer, L. L. & Morikawa, G. K. 1976 Stability of rectilinear geostrophic vortices in stationary equilibrium. *Phys. Fluids* **19**, 929–942.

Burbea, J. 1982 On patches of uniform vorticity in a plane irrotational flow. *Arch. Rat. Mech. Anal.* **77**, 349–358.

Campbell, L. & Ziff, R. 1978 A catalog of two-dimensional vortex patterns. Los Alamos Scientific Laboratory, Rep. No. LA-7384-MS.

Carnevale, G. F. & Kloosterziel, R. C. 1994 Emergence and evolution of triangular vortices. *J. Fluid Mech.* **259**, 305–331.

Carton, X. & Legras, B. 1994 The life-cycle of tripoles in two-dimensional incompressible flows. *J. Fluid Mech.* **267**, 53–82.

Crowdy, D. G. 1999 A class of exact multipolar vortices. *Phys. Fluids* **11**, 2556–2564.

Davis, P. J. 1974 *The Schwarz Function and its Applications*. Carus Mathematical Monographs.

Deem, G. S. & Zabusky, N. J. 1978 Vortex waves: stationary V-states, interactions, recurrence and breaking. *Phys. Rev. Lett.* **40**, 859–862.

Dritschel, D. G. 1985 The stability and energetics of co-rotating uniform vortices. *J. Fluid Mech.* **157**, 95–134.

Dritschel, D. G. 1986 The nonlinear evolution of rotating configurations of uniform vorticity. *J. Fluid Mech.* **172**, 157–182.

Dritschel, D. G. 1988*a* The repeated filamentation of two-dimensional vorticity interfaces. *J. Fluid Mech.* **194**, 511–547.

Dritschel, D. G. 1988*b* Contour surgery: a topological reconnection scheme for extended interactions using contour dynamics. *J. Comput. Phys.* **77**, 511–547.

Durkin, D. & Fajans, J. 2000 Experiments on two-dimensional vortex patterns. *Phys. Fluids* **12**, 289–293.

Fine, K., Cass, W., Flynn, W. & Driscoll, C. F. 1995 Relaxation of 2D turbulence to vortex crystals. *Phys. Rev. Lett.* **75**, 3277.

Havelock, T. H. 1931 The stability of motion of rectilinear vortices in ring formation. *Phil. Mag.* (Series 7) **1**, 617–633.

Kelvin, W. T. 1878 *Mathematical and Physical Papers*, vol. 4, p. 135. Cambridge University Press.

Khazin, L. G. 1976 Regular polygons of point vortices and resonance instability of steady states. *Sov. Phys. Dokl.* **21**, 567–569.

Legras, B. & Dritschel, D. G. 1991 The elliptical model of two-dimensional vortex dynamics. *Phys. Fluids* A **3**, 845–854.

Meiron, D. I., Saffman, P. G. & Schatzmann, J. C. 1984 The linear two-dimensional stability of inviscid vortex streets of finite-cored vortices. *J. Fluid Mech.* **147**, 187–212.

Mertz, G. 1978 Stability of body-centered polygonal configurations of ideal vortices. *Phys. Fluids* **21**, 1092.

Morel, Y. G. & Carton, X. J. 1994 Multipolar vortices in two-dimensional incompressible flows. *J. Fluid Mech.* **267**, 23.

Morikawa, G. K. & Swenson, E. V. 1971 Interacting motion of rectilinear geostrophic vortices. *Phys. Fluids* **14**, 1058–1073.

Overman, E. A. 1986 Steady-state solutions of the Euler equations in two dimensions II: local analysis of limiting V-states. *SIAM J. Appl. Maths* **46**, 765–800.

Polvani, L. M. & Carton, X. 1990 The tripole: a new coherent structure of incompressible two-dimensional flows. *Geophys. Astrophys. Fluid Dyn.* **51**, 87–102.

Polvani, L. M. & Dritschel, D. G. 1993 Wave and vortex dynamics on the surface of a sphere. *J. Fluid Mech.* **255**, 35–64.

Pullin, D. I. 1992 Contour dynamics methods. *Annu. Rev. Fluid Mech.* **24**, 89–115.

Saffman, P. G. 1992 *Vortex Dynamics*. Cambridge University Press.

Thomson, J. J. 1882 *On the Motion of Vortex Rings* (Adams Prize Essay, 1882). Macmillan, 83 pp.

Yarmchuk, E. J., Gordon, M. J. & Packard, R. E. 1979 *Phys. Rev. Lett.* **43**, 214–217.